

## FIFTH AUSTRALASIAN CONFERENCE

on

## HYDRAULICS AND FLUID MECHANICS

at

University of Canterbury, Christchurch, New Zealand

December 9 to December 13 1974

MODELLING THE AIRFLOW OVER AND TO THE LEE OF THE  
SOUTHERN ALPS, NEW ZEALAND

N. J. Cherry

The uses and limitations of single and multilayer linearised analytic models of the airflow over and to the lee of complex mountain ranges are discussed with applications to the Southern Alps. Comparisons between the models are made to determine their usefulness in forecasting. It is found that in some cases although the flow to the lee of the mountains looks real, the flow over the mountains, due to the superposition of several modes from several mountains, reaches very large amplitudes. These are not observed in practice and are in conflict with the linearising assumption of 'small' amplitude perturbations. They may however be indicative of severe turbulence over the mountains and still be useful in forecasting.

Department of Agricultural Engineering,  
Lincoln College, Canterbury, N.Z.

## Glossary of terms

a, b	the half-width and height of the model bell shaped mountain,
c	the speed of sound,
g	the acceleration due to gravity,
$\Gamma$	the dry adiabatic lapse rate ( $9.76 \text{ }^\circ\text{K km}^{-1}$ ),
$h_i$	the heights of the interfaces between the model layers, $i=1, 2, \dots, N$
H	the height of the upper boundary,
$J_p(X), Y_p(X)$	Bessel functions of the first and second kind, respectively, of order p and argument X,
k	the horizontal wavenumber of the lee wave, 'r' refers to a particular solution,
$l^2$	Scorer's parameter, a measure of dynamic stability,
U, $\rho$ , T, $\gamma$	the mean flow horizontal wind speed, density, temperature and lapse rate,
w, D	the vertical perturbation velocity and displacement from the equilibrium level,
x, z	the horizontal and vertical coordinates,
(')	the prime refers to differentiation with respect to z.

## 1. Introduction

The waves that form to the lee of mountains are important mainly because of the effect on aircraft of the turbulence associated with them. They also cause some damage on the ground when they produce high surface wind speeds. Often the presence of waves can be seen in the cloud structure. However they exist in the clear air also so it is essential that their formation can be forecast so that pilots can be warned of levels where clear air turbulence (CAT) may be expected.

This may be approached in two ways. First by summarizing many observations to give the characteristics of the airflows for which large amplitude lee waves have been observed over a particular location. This was done for example, by Cherry (1972) who observed that when large amplitude lee waves were observed over Christchurch the following conditions were generally fulfilled:

- The mean tropospheric wind direction was within the angular range of the mountain ridges upstream of Christchurch. That is from between  $290^\circ$  and  $340^\circ$ , which is within  $30^\circ$  of the direction perpendicular to the mean direction of the Southern Alps in the vicinity,  $310^\circ$ .
- The wind speed at the level of the mountain ridges (approx. the 800 mb level) was in excess of  $10 \text{ m sec}^{-1}$ .
- The mean tropospheric wind speed was in excess of  $20 \text{ m sec}^{-1}$ .

These are consistent with the observations of Gerbier and Berenger (1960) and the theoretical conclusions of Scorer (1949).

A second way is to have a reliable model that will give to a good approximation the scale of the vertical disturbance to be expected at any level that aircraft may fly at over the mountains and to their lee. The aim of this paper is to explore some of the potentialities and limitations of linearised analytic models in this respect.

## 2. Linear analytic lee wave theory

Perturbation theory is used with the equations of motion, the hydrostatic, continuity and isentropic equations to derive the linearised wave equation, Yih (1965),

$$\nabla^2 w - \beta w' + \left( \frac{g\beta_1}{U^2} - \frac{U''}{U} \right) w = 0 \quad (1)$$

in which  $\nabla^2 = \frac{\partial^2}{\partial x^2} + \frac{\partial^2}{\partial z^2}$ ,  $\beta = \frac{\rho'}{\rho}$  and  $\beta_1 = \beta - \frac{g}{c^2} = \frac{1}{T}(\Gamma - \gamma)$

the coefficient of w is known as Scorer's parameter,  $l^2$ . Now the linearised equation for a streamline gives

$$U \frac{\partial D}{\partial x} = w \quad (2)$$

Assuming that  $w$  and  $D$  have the form

$$w = w(z) e^{ikx}, \quad D = D(z) e^{ikx} \quad (3)$$

Eq. 1 can be written

$$D''(z) + (2\alpha - \beta) D'(z) + \left( \frac{g\beta^2}{U^2} - k^2 \right) D(z) = 0 \quad (4)$$

where  $\alpha = \frac{U'}{U}$ . Scorer (1969) showed that this equation may be used to describe large amplitude lee waves as long as the streamlines are not too steep. That is as long as  $(2g/c^2)D \ll 1$  or  $D \ll 5$  km. If we assume that the lower boundary is a bell shaped mountain, i.e.

$$D(0) = \frac{a^2 b}{a^2 + x^2} = ab \int_0^\infty \cos kx e^{-ka} dk \quad (5)$$

we obtain an analytic solution of the wave equation, namely

$$D(x, z) = A(z) \begin{cases} x > 0 & \left\{ B(x) \frac{\Psi_i(k_0, z)}{\Psi_i(k_0, 0)} + \frac{\Psi_i(k_r, z)}{\frac{d}{dk} \Psi_i(k_r, 0)} \right. \\ x \leq 0 & \left. B(x) \frac{\Psi_i(k_0, z)}{\Psi_i(k_0, 0)} \right. \end{cases} \quad (6)$$

The first term is the mountain disturbance and the second term is the lee wave term. The final solution will include the sum of the mountain disturbance of each of the mountains and the sum of all the lee wave terms for each of the resonant modes, if there are any. Now in Eq. 6,

$$\begin{aligned} A(z) &= ab \frac{U(0)}{U(z)} \left( \frac{\beta(0)}{\beta(z)} \right)^{\frac{1}{2}} \\ B(x) &= \frac{a}{a^2 + x^2} \\ C(x) &= -2\pi e^{-k_r a} \sin k_r x \end{aligned} \quad (7)$$

The parameter  $\Psi$  is a solution of the transformed linearised wave equation

$$w'' + (l^2 - k^2) w = 0 \quad (8)$$

under the assumed boundary conditions. It is also assumed that  $w$  and  $w'$  are continuous across the layer interfaces.

If  $l^2$  is constant within each layer then in the  $i$ th layer

$$\Psi_i(k, z) = \cosh \mu_i(z - h_i) + Q_i \sinh \mu_i(z - h_i) \quad (9)$$

where

$$\mu_i = (k^2 - l_i^2)^{\frac{1}{2}} = -i(l_i^2 - k^2)^{\frac{1}{2}}$$

The  $Q_i$ 's are determined by the boundary and interface conditions and in the mountain disturbance term  $k_0 = 0$ .

If  $l^2$  varies exponentially with height within each layer, say

$$l^2 = B_0 e^{-\lambda z} + B_1 \quad (10)$$

$\Psi$  has the general form

$$\Psi(k, z) = J_\nu(P(z)) + Q_i K Y_\nu(P(z)) \quad (11)$$

where

$$\begin{aligned} P(z) &= \frac{2}{\lambda} B_0^{\frac{1}{2}} e^{-\lambda z} \\ K &= \frac{J_\nu(p(H))}{Y_\nu(p(H))} \\ k &= (B_1 + (\frac{\lambda \nu}{2})^2)^{\frac{1}{2}} \end{aligned} \quad (12)$$

In the mountain disturbance term in Eq. 6,  $k_0 = B_1^{\frac{1}{2}}$  ( $\gamma = 0$ ). The wave numbers of the resonant lee wave modes, if there are any, are found from the solution of

$$\Psi_1(k, z) = 0 \quad (13)$$

### 3. Discussion of the models

The characteristics of the models are initially best seen through a discussion of the properties of one and two layer models. The characteristics of a single unbounded exponential layer model were discussed by Döös (1961). For an unbounded model  $K = 0$  in Eq. 11, hence the wavenumbers of the lee waves are found from the solutions of

$$J_\nu(\beta) = 0 \quad (14)$$

where

$$\beta = \frac{2}{\lambda} B_0^{\frac{1}{2}}$$

The number of roots is determined by  $\beta$  which is a function of the vertical variation of the wind speed and the stability. From Jahnke and Emde (1948) we find that:

$0 \leq \beta < 2.405$	no waves
$2.405 \leq \beta < 5.520$	one wave mode
$5.520 \leq \beta < 8.654$	two wave modes
$8.654 \leq \beta < 11.792$	three wave modes
⋮	⋮
⋮	⋮
⋮	⋮

The usual variation of wind and stability in the troposphere generally results in up to two lee wave modes. The sum of  $B_0$  and  $B_1$  is equal to the assumed boundary layer  $l^2$  value.  $B_1$  is generally small and is approximately equal to the value of  $l^2$  high in the troposphere. Hence for waves to exist  $l^2$  must be sufficiently large near the ground and be accompanied by a sufficiently small rate of decrease in  $l^2$  with height that  $\beta$  exceeds 2.405. Even if the low level air is very stable ( $B_0$  is large) wave formation can be inhibited if the air's dynamic stability decreases too quickly with height ( $\lambda$  is too large). From Eq. 12 we can see that there are no solutions for wavenumbers less than  $B_1^{\frac{1}{2}}$ . We find this in all the models that the longest wavelength that can be produced is limited by the lowest stability.

For Scorer's unbounded two layer model with  $l^2$  constant in each layer, Eq. 11 becomes

$$\tanh \mu_1 h_1 = - \frac{\mu_1}{\mu_2} \quad (15)$$

This has  $N$  discrete solutions if

$$(l_1^2 - l_2^2) h_1 \geq (2n + \frac{1}{2}) \quad (16)$$

$n = 0, 1, 2, \dots, N-1.$

Again there are no solutions for  $k < l_2$ , the value in the upper layer. The results expressed by Eq. 16 are consistent with the exponential model in that the low level dynamic stability ( $l_1^2$ ) must exceed the upper level dynamic stability by a sufficient amount and the rate of decrease of  $l^2$ , being inversely proportional to  $h_1$ , also limits the number of modes.

On the 15th July 1970 a superpressure balloon was released from Birdlings Flat and showed evidence of lee waves in the southwesterly airflow to the lee of Banks Peninsula. The airflow characteristics for midday on this day are shown in Fig. 1. The dip in the wind speed profile at around 3 km is a rather unusual feature and caused the deep stable surface layer. The  $l^2$  profile was approximated by two layers as shown. Fig. 2 shows the mountain and balloon profiles with the model solution for the lee flow near the level of the balloon. The amplitudes compare very favorably. We shall see later that the longer wavelength of 12 km that was observed could be the result of the stable upper layer which this model ignores.

On the 15th October 1970 a strong northwesterly was blowing. A balloon was released from Hokitika at 7am. It was picked up by the balloon tracking meteorological radar at Harewood and tracked as it traced the lee flow, Fig. 3. The large oscillations over the Alps may indicate large amplitude oscillations of the air but they are likely to have been strongly accentuated by radar reflections from the Alps at low elevations which can cause the radar to fluctuate between the balloon signal and the ground reflection. A power spectrum analysis of the balloon profile to the lee of the mountains indicates

that there are two modes superimposed. These have wavelengths of about 2 and 12 km. A satellite photograph taken at 1625 shows well developed waves extending at least 150 km downstream of the mountains between Canterbury and East Cape. Their mean wavelength is about 11.5 km. The complex profile of the mountain cross-section was approximated by 10 bell shaped mountains, Fig. 4. The airflow characteristics for midday, derived from the Harewood rawinsonde flight, Fig. 5, are typical of airflows that support wave formation. The wind speed increases strongly through the troposphere, causing  $l^2$  to decrease from its low level maximum value. Close to the tropopause  $U$  reaches its maximum and decreases quickly into the stratosphere, combining with the static stability to form a very dynamically stable layer. The  $l^2$  profile was averaged over 1 km layers, the broken line showing averaging centred on each km level.

An inconsistency arises with the use of the observed airflow profiles alongside the model parameters in the amplitude calculation. To gauge the significance of this a modified temperature  $T'$  was calculated.  $T'$  is the temperature that would be required, together with the observed wind speed profile, to give the model  $l^2$  profile, in this case an exponential, Fig. 5. Throughout most of the troposphere the difference is small.

The exponential model has two solutions, wavelengths of 14.7 and 10.1 km. The waves both reach a maximum positive amplitude near 2 km AGL. The longer wavelength wave has a nodal surface near 4km and a negative amplitude above this height. The shorter wavelength wave remains constant but decreases to be quite small above 10 km. The maximum amplitude would occur near 2 km and would be about 1700 m if the mountains were all in phase. The lee flow resulting from the superposition of all the wave trains, Fig. 7, has an amplitude of about 400 m indicating that there is considerable destructive interference in the periodic forcing of the mountains.

Another method was used to give a better fit of the exponential to the  $l^2$  profile. This gave a single solution of 9.3 km. This has the same amplitude characteristics with height as the shorter wavelength above but was in better resonance with the individual mountains. The maximum possible lee wave amplitude would be about 8.5 km but again destructive interference results in a maximum amplitude to the lee of 590 m. The amplitude at the level of the balloon was about 250 m, less than that observed.

#### 4. Stratospheric stability and the upper boundary

In many cases it may be appropriate to approximate the tropospheric  $l^2$  profile by an exponential of two layer profile, but these ignore the effect of the stratosphere which is usually very statically and dynamically stable. The effect of the stratospheric stability can be seen in Cherry (1971) in which an analysis of radiosonde soundings from Harewood during northwesterly winds is given. Anomalous vertical velocities (departures from the mean ascent rate) are calculated as well as the  $l^2$  profiles. The most common form of profile shows  $l^2$  decreasing above the stable surface layer, which is 1 to 3 km deep, to be quite small up to around 10 km. About this level  $l^2$  increases slowly with height up to about 15 to 18 km at which point it starts to increase very quickly with height. This profile usually results in lee waves throughout the troposphere with a low level maximum amplitude for the short wavelength waves. Often there is an enhancement of the amplitude, particularly of the long wavelength waves if there are any, between 10 and 15 km where  $l^2$  is increasing slowly with height. The amplitude becomes small above this height but sometimes becomes large again in the very stable layer above. There are two cases where  $l^2$  remains small but fairly constant above 15 km and there are no large waves above this level. On the one occasion when  $l^2$  decreased above this level a very large amplitude wave was observed.

It is found, Cherry (1971), that there is very little difference in the wavelengths that result from including either a very stable third layer above 15 km or a rigid upper boundary at that level. However the effect of both of these is to produce a new long wavelength solution which has small amplitude at low levels and a larger amplitude in the upper troposphere and low stratosphere, Corby and Sawyer (1958). The shorter wavelength is left unaffected as it has a very small amplitude at the levels where the stable layer or the upper boundary have been placed.

The effect of a rigid upper boundary in the models is to change  $Q_N$ , where  $N$  refers to the top layer. From Eq. 9 we see that setting  $\Psi_N(k, H)$  to zero gives

$$Q_N = -\coth \mu_N H \quad (17)$$

Now  $Q_N \rightarrow -1$  when  $(\mu_N H) \gg 1$ , which is consistent with the unbounded model. The rest of the

Q's follow from the interface continuity conditions and the lower boundary condition. The effect of an upper boundary and a stable stratospheric layer can be seen in Fig. 7, which shows a bounded four layer solution for the 15th October 1970. The  $l^2$  profile was averaged over 4 km layers with a rigid upper boundary at 16 km. The surface layer is very stable and the flow in it is dominated by the 8.1 km wavelength lee wave. In the middle two less stable layers the longer 19.8 km wavelength reaches a maximum amplitude and dominates the upper tropospheric flow. The interface below the very stable stratospheric layer produces a nodal surface. This shows how the same tropospheric solution could be obtained if there was a rigid boundary at this level. However the fourth layer shows the existence of large amplitude stratospheric lee waves which are reversed in phase. The flow close to the mountains where the streamlines intersect indicates that the linear theory is breaking down. However it is probably indicative of severe turbulence at these locations. The low level lee flow shows a situation in which high surface winds would be experienced, especially near 108, 125 and 165 km.

## 5. Conclusions

The solutions of models with a small number of layers give a good indication of the scale of vertical motion to be expected from complex mountain ranges such as the Southern Alps. It is important to include the effects of the stable stratospheric layer. If the troposphere only is of interest this may be done by placing a rigid upper boundary in the low stratosphere where  $l^2$  is increasing with height. Lee waves in the low stratosphere can be seen if a stable layer is used. Large amplitudes can be produced over the mountains that the linear theory cannot handle properly. These can still be used as indicators of the presence of turbulence. For the scale of wavelengths usually observed (6 to 30 km) the periodic forcing of successive ranges of mountains can produce larger amplitudes than an individual mountain but across the whole system of mountains that form the Southern Alps there is a good deal of destructive interference which results in realistic amplitudes to the lee of the mountains.

## REFERENCES

- Cherry, N.J., 1971: "A study of winds and waves", unpublished Ph.D. thesis, lodged in the library of the University of Canterbury, New Zealand.
- Cherry, N.J., 1972: "Winds and lee waves over Canterbury, New Zealand, during 1970", N.Z. J. Sci., 15, pp 585-600.
- Corby, G.A. and Sawyer, J.S., 1958: "The airflow over a ridge: the effects of the upper boundary and high level conditions", Quart. J.R.Met.Soc., 84, pp 25-37.
- D88s, B.O., 1961: "A mountain wave theory including the effects of the vertical variation of the wind and stability", Tellus, 13, 3, pp 305-319.
- Gerbier, N. and Berenger, M., 1960: "Experimental studies of lee waves", Quart. J. R. Met. Soc., 86, pp 13-21.
- Jahnke, E. and Emde, E., 1948: "Tables of functions with formulae and curves", Fourth Edition, Dover Publications, New York.
- Scorer, R.S., 1949: "Theory of waves in the lee of mountains", Quart. J. R. Met. Soc., 75, pp 41-59.
- Scorer, R.S., 1969: "Present state of theory of large amplitude oscillations in stratified fluids", Internal gravity and acoustic waves - a colloquium. NCAR-TN-43, National Center for Atmospheric Research. Boulder, Colorado.
- Yih, C.S., 1965: "Dynamics of Nonhomogeneous Fluids", MacMillan Co., New York, 306pp.

Fig. 1: The airflow profiles for 15th July 1970. The  $1^2$  profile and the two layer model approximation are given on the right.

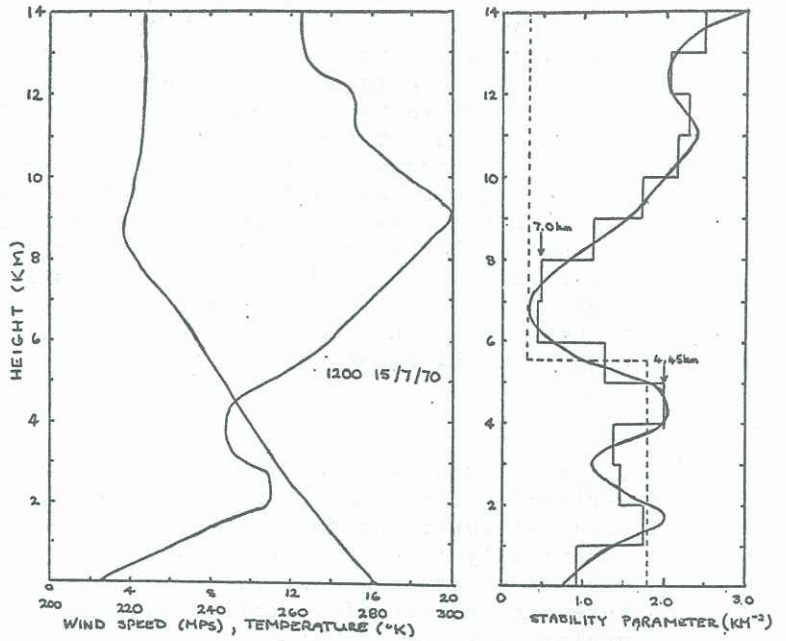


Fig. 2: The balloon and mountain profiles for 15th July, 1970, with the lee flow solution near the balloon's equilibrium level.

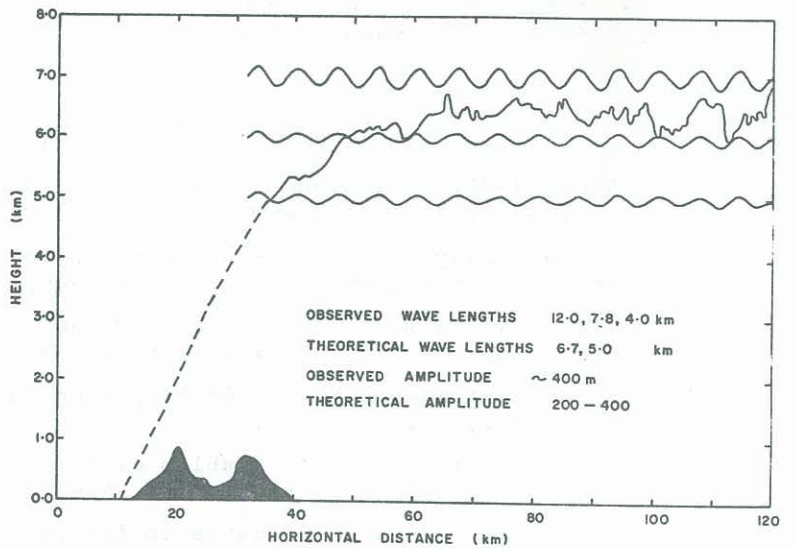
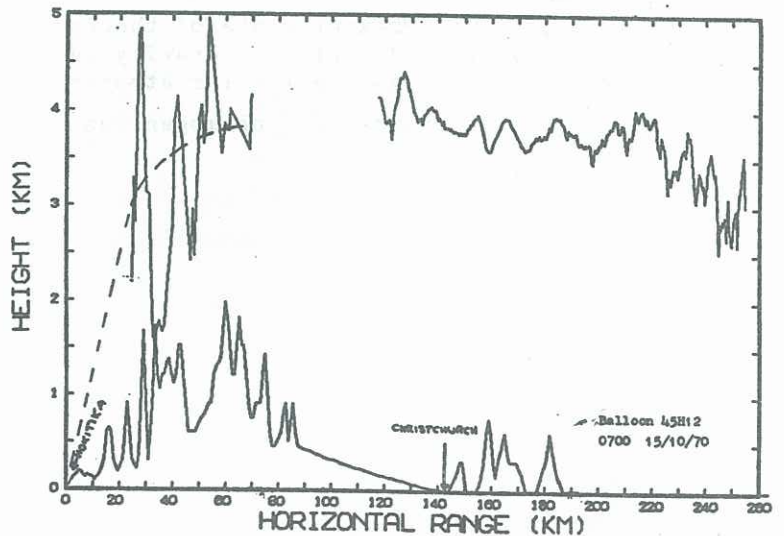


Fig. 3: The balloon and mountain profiles for a superpressure balloon released from Hokitika at 7 am on 15th October 1970.



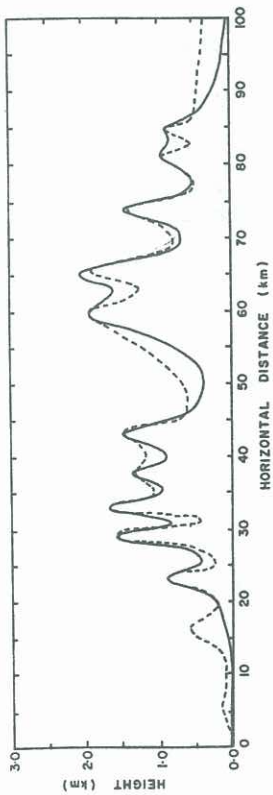


Fig. 4: The mountain profile (broken line) and the approximate model mountain profile (solid line) constructed using 10 bell shaped mountains.

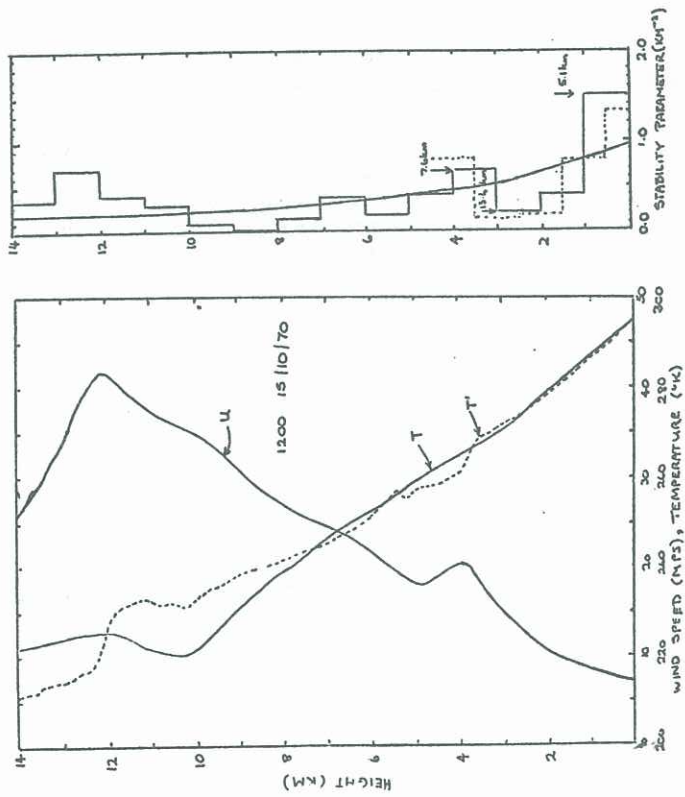


Fig. 5: The airflow characteristics from the 1200 15th October 1970 Harewood rawinsonde sounding, with the  $l^2$  profiles averaged over 1 km layers and the fitted exponential model profile.

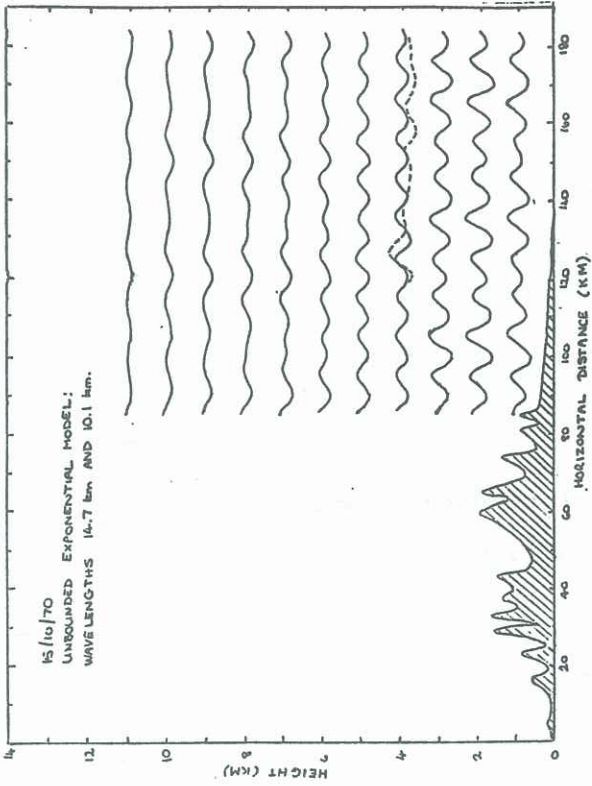


Fig. 6: The lee wave flow for the unbounded exponential model for 15/10/70. The broken line is the balloon trace.

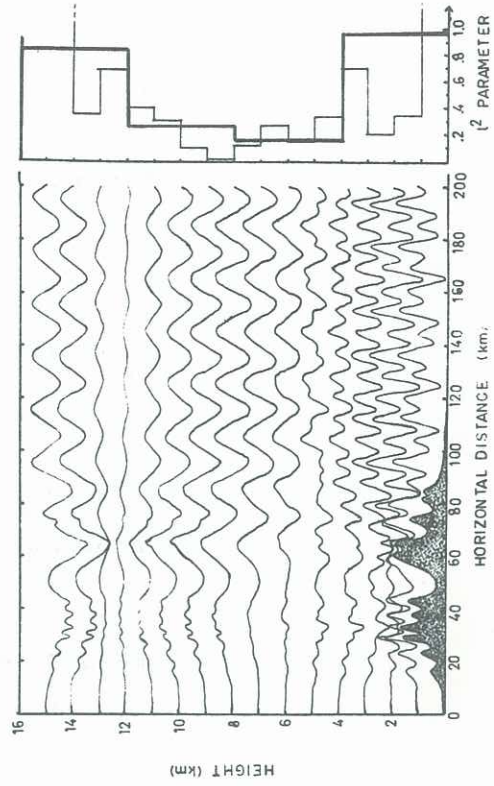


Fig. 7: The flow over and to the lee of the mountains for the 4 layer, constant  $l^2$  model for 15/10/70, bounded at 16 km. There are two resonant modes, 19.8 and 8.1 km.